ELSEVIER

PII: S0963-8695(98)00013-9

NDT&E International, Vol. 31, No. 4, pp. 289–297, 1998
© 1998 Elsevier Science Ltd. All rights reserved
Printed in Great Britain
0963-8695/98 $19.00+0.00

Characterisation of surface cracks with Rayleigh waves: a numerical model

G. Hévin[a,*], O. Abraham[a], H. A. Pedersen[b], M. Campillo[b]

[a]Laboratoire Central des Ponts et Chaussées, Centre de Nantes, Bouguenais, France
[b]Laboratoire de Géophysique Interne et Tectonophysique, Université Joseph Fourier, Grenoble, France

In the non-destructive testing of concrete structures, the use of Rayleigh waves shows some advantages to characterise surface cracks: easiness of excitation and recording, access to only one surface of the structure required, great spectral sensitivity to the propagation medium.... But the behaviour of Rayleigh waves on surface defects in concrete is difficult to perceive in the field, even if the dependence of the diffraction pattern on the crack's geometrical features is significant.

A numerical model is adapted from earth physics in order to better understand the influence of the crack geometry on Rayleigh-wave propagation. This model, based on an indirect boundary element method, calculates the three-dimensional seismic response of two-dimensional structures. Synthetic seismograms are obtained for the propagation of a Rayleigh wave across various crack geometries. The variations of spectral ratios between the transmitted and incident waves are studied as a function of the crack depth. They are used to design an efficient procedure for the determination of crack depths. © 1998 Elsevier Science Ltd. All rights reserved

Keywords: Rayleigh waves, surface cracks, concrete, IBEM

Introduction

All structures are submitted to weathering. As a consequence, civil engineers are faced with the problem of sounding buildings and evaluating the importance of alteration[1–3]. One objective is to quantify damages that affect the mechanical behaviour of the whole structure. In this domain the detection and characterisation of surface cracks and faults are particularly important. Non-destructive techniques try to answer this question using different physical phenomena (optical diffraction, ultrasonics, electrical methods, radiographic inspection)[4]. The use of surface waves seems to be a promising tool for studying concrete structures because this type of surface waves, and especially Rayleigh waves (R-waves), fulfil many non-destructive testing requirements.

* Address for correspondence: G. Hévin, Laboratoire Central des Ponts et Chaussées, Centre de Nantes, BP 19, F 44340 Bouguenais, France.

When a R-wave propagates, the particle path is a retrograde ellipse in the vertical plan[5]. The primary feature of R-waves, like other surface waves, is that the whole energy propagates near the free surface, parallel to it. Surface sources radiate high amounts of R-waves. Miller and Pursey[6] evaluated that a point force in a homogeneous half-space radiates 67% of the energy as a Rayleigh wave while 26% is carried by the shear wave and 7% by the compression wave. Moreover, surface waves propagate radially along a circular wave front on the surface. Consequently, on the surface, the attenuation of this wave by geometrical spreading is smaller than that of body waves with their spherical wave front. Because of all these features, R-waves are particularly energetic and thus 'easy' to excite and to record. Another advantage is that the only necessary access is the surface under study.

The real interest of R-waves is their sensitivity to the medium in which they propagate. Their depth of propagation depends on the wavelength. Thus, for a medium with a

velocity varying with depth, the R-wave velocity depends on the frequency. This is the dispersion phenomenon. The dispersion and diffraction patterns of these waves can supply a lot of information on the propagation medium. The aim of this paper is to evaluate the ability of R-waves to fulfil the needs of civil engineers in the investigation of surface cracking. This study of R-waves leads us to suggest several tools in the experimental and numerical fields.

Rayleigh waves in the field

Seismologists were the first to work on R-waves. In exploration seismology, their interest was due to the fact that R-waves were considered as noise on seismic records (ground roll) which had to be removed to enhance the desired signal[7]. Studies led geophysicists to better understand the behaviour of these waves. Indeed, the dispersion of R-waves makes it possible to determine seismic velocities for multilayered media[5]. Good results have been obtained in soils on small and large scales and signal processing techniques keep improving[5,8–11]. Knowledge of the earth's geophysics provides a good basis for developing new non-destructive techniques.

In the non-destructive field, the detection and characterisation of surface cracks with R-waves was first widely developed for metallic materials with ultrasonics techniques[4,12,13]. Previous studies provide several hypotheses on the diffraction patterns of R-waves on surface defects. To summarise, surface cracks can be viewed as reflectors, low-pass filters and delay gates. The diffraction pattern makes the sizing of cracks possible by the spectral analysis[14] or the study of the arrival time of each wave train[13,15] i.e., the reflected wave, the low frequency transmitted wave and the delayed transmitted wave (Figure 1).

Note also the work on the use of trenches for seismic wave isolation. To attenuate selected frequency bands, the effectiveness of such trenches depends strongly on the behaviour of the R-waves on these trenches and on their spectral analysis[16,17].

All these studies provide a good basis to carry out experimental tests on a concrete slab to evaluate the adequacy of the diffraction theory to the small scale structures of civil engineering.

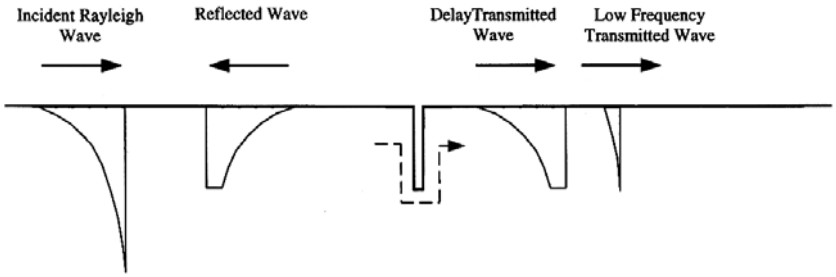

Figure 1 Interaction of a R-wave on a surface crack (from Ref. [13])

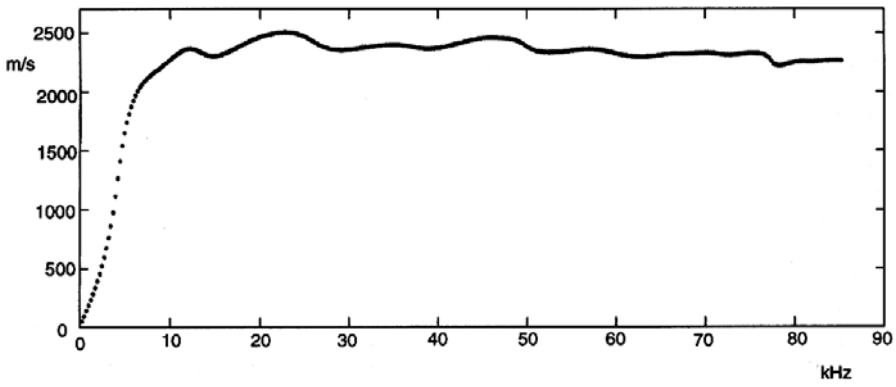

Figure 2 Dispersion curve obtained from the unwrapped phase by the SASW method on an homogeneous concrete slab

Experimental tests

In the first step, we determined the velocities of R-waves in a sound concrete slab of 4 × 4 m and thickness 0.4 m. Recordings were carried out with Brüel & Kjaer piezo-accelerometers n°4381 connected to a digital acquisition system. An impact on the surface of the slab, obtained with a steel ball controlled with an electromagnet, generated the R-waves. The Spectral Analysis of Surface Wave method[9,18] was used to determine the dispersion curve (Figure 2). This method consists of measuring the phase shift between signals recorded at two different locations for the same impact. After unwrapping this phase shift and determining the distance between the two sensors, the phase velocity of the R-wave is evaluated for each frequency. As predicted, the phase velocity appears globally constant (around 2300 m s^{-1}) for the whole frequency band (from 5 to 80 kHz): the concrete slab is a non-dispersive medium for wavelengths from 2 to 40 cm.

In the second step, an artificial crack was introduced in the slab and a second set of measurements was carried out. These tests have revealed that experimental data are very noisy because concrete is a non-homogeneous medium so the noise produced by scattering from the microstructure is significant. Moreover, because the surface of the concrete slab is not perfectly flat, it is very difficult to get a repeatable source in amplitude. If several tests confirm the great sensitivity of R-waves to the presence of the crack, the accuracy is not sufficient to apply a time domain analysis as commonly undertaken in homogeneous media like metal[13,15].

A better knowledge of the behaviour of R-waves on a surface crack appears necessary. To understand the scattering phenomena due to a crack, numerical simulations of wave propagation on such a geometry may provide the missing information for an accurate interpretation of the experimental tests.

Numerical model

Theoretical aspects

During the last two decades, numerical simulation methods of wave propagation have greatly improved. While analytical calculations make it possible to solve many simple problems, new numerical methods, with the development of computers, are nowadays very efficient for complex geometries. However, if two-dimensional wave fields have been numerically modelled by numerous authors[19], numerical calculation for three-dimensional problems[20] still requires a significant amount of computer memory and calculation time.

A collaboration between the Laboratoire de Géophysique Interne et Tectonophysique (Grenoble, France) and the Laboratoire Central des Ponts et Chaussées (Nantes, France) resulted in a program of numerical simulations in concrete structures with a code adapted from earth physics. This code calculates the three-dimensional wave response of two-dimensional geometries by means of the Indirect Boundary Element Method (IBEM). IBEM is based on the representation theorem[5]. From this theorem, the wave field in an elastic medium can be written as the superposition of the radiations from sources located on the interface of the model. The displacement field in an elastic domain V with a boundary S can be written as

$$u_i(x) = \int_s \psi_j(\zeta) G_{ij}(x, \zeta)\, \mathrm{d}S_\zeta \tag{1}$$

where $u_i(x)$ is the ith component of displacement at x, $G_{ij}(x,\zeta)$ is the Green function, i.e., the displacement in direction i at x due to a point force in direction j applied at the point ζ and $\psi_j(\zeta)$ is the force density in direction j at ζ. By convention, we will use in all these equations the sum on common subscripts. The integral representation makes computation of stresses and tractions possible by the application of Hooke's law. However, special care must be taken at boundary singularities (when $x = \zeta$ on the boundary). By a limiting process based on equilibrium considerations around an internal neighbourhood of the boundary, it is possible to write for x on S that[21]

$$t_i(x) = c\psi_i(x) + \int_s \psi_j(\zeta) T_{ij}(x, \zeta)\, \mathrm{d}S_\zeta \tag{2}$$

where $t_i(x)$ is the ith component of traction at x, c equals 0 if x is outside S, 1/2 if x tends to S from the inside of V and $-1/2$ if x tends to S from the outside of V. $T_{ij}(x,\zeta)$ is the traction Green function, i.e., the traction in direction i at x of a point source in direction j applied at the point ζ. T_{ij} is found by application of Hooke's law to Equation (1).

For the calculations the surface is discretized into N segments of length ΔS. Discrete expressions are used

$$u_i(x_n) = \sum_{k=1}^{N} \psi_j(\zeta_k) g_{ij}(x_n, \zeta_k) \tag{3}$$

$$t_i(x_n) = \sum_{k=1}^{N} \psi_j(\zeta_k) g_{ij}(x_n, \zeta_k) \tag{4}$$

with

$$g_{ij}(x_n, \zeta_k) = \int_{\zeta_k - \Delta s/2}^{\zeta_k + \Delta s/2} G_{ij}(x_n, \zeta_k)\, \mathrm{d}S_\zeta \tag{5}$$

$$t_{ij}(x_n, \zeta_k) = \int_{\zeta_k - \Delta s/2}^{\zeta_k + \Delta s/2} (c\delta_{ij}\delta(x_n - \zeta_k) + T_{ij}(x, \zeta_k))\, \mathrm{d}S_\zeta \tag{6}$$

The free field (u^o, t^o) is defined as the displacements and tractions due to incident waves without the irregularity. The ground motion is the superposition of the free field and the diffracted wave field that follows Equation (3). Thus, the

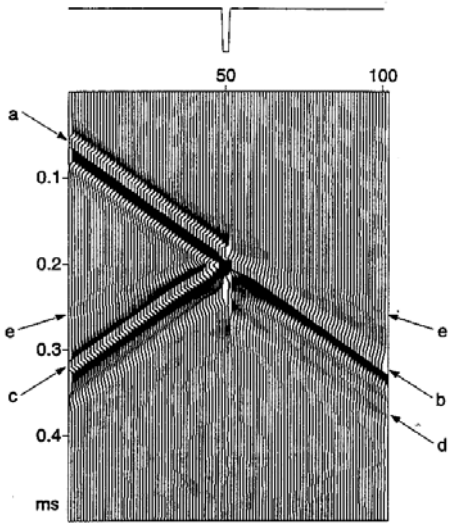

Figure 3 Synthetic seismograms (vertical component) for a crack of 5 cm depth: (a) incident R-wave (Ricker pulse); (b) direct transmitted R-wave; (c) reflected R-wave; (d) delayed transmitted R-wave; (e) body wave from conversion mode of R-wave

total displacements and tractions are

$$u_i(x_n) = u_i^0 + \sum_{k=1}^{N} \psi_j(\zeta_k) g_{ij}(x_n, \zeta_k) \tag{7}$$

$$t_i(x_n) = t_i^0 + \sum_{k=1}^{N} \psi_j(\zeta_k) t_{ij}(x_n, \zeta_k) \tag{8}$$

Three boundary conditions must be satisfied:

(1) tractions equals 0 at free surfaces;

(2) displacements and tractions are continuous across interfaces;

(3) the total field equals 0 at infinity. From condition 1, Equation (8) can be written as:

$$\sum_{k=1}^{N} \psi_j(\zeta_k) t_{ij}(x_n, \zeta_k) = -t_i^0(x_n) \; n = 1, \ldots, N \tag{9}$$

This linear system of equations is solved and displacements are calculated with Equation (7). IBEM uses compact expressions of the Green functions appropriate to this type of problem. A detailed discussion of this method and its applications in site effect simulations can be found in Refs [21,22]. Highly accurate results are produced at a low computational cost. The Green's function used makes it possible to consider waves upon the two-dimensional crack, so the diffracted wave-field is three-dimensional.

Calculations of synthetic seismograms for surface crack geometries

The calculations are performed for an incidence perpendicular to the crack. The program considers a half-space with a surface crack of infinite length (Figure 3). Its width is 5 mm and the depth takes different values: 5, 10 and 15 cm. The medium is characterised by Poisson's ratio of $\nu = 0.30$ and S-wave velocity of $\beta = 2500$ m s^{-1}, as evaluated from experimental measures. The surface of the half space and the edges of the crack are free. Results are presented as synthetic seismograms (Figures 3 and 4). They show the response of 101 pseudo-displacement-sensors located along the profile. The incident R-wave is a Ricker pulse with a central frequency of 30 kHz.

For a 5-cm crack depth, three wave trains are clearly seen: the incident wave (Figure 3*(a)*), the direct transmitted wave (Figure 3*(b)*) and the reflected wave (Figure 3*(c)*). As the whole displacement field is calculated, conversion mode

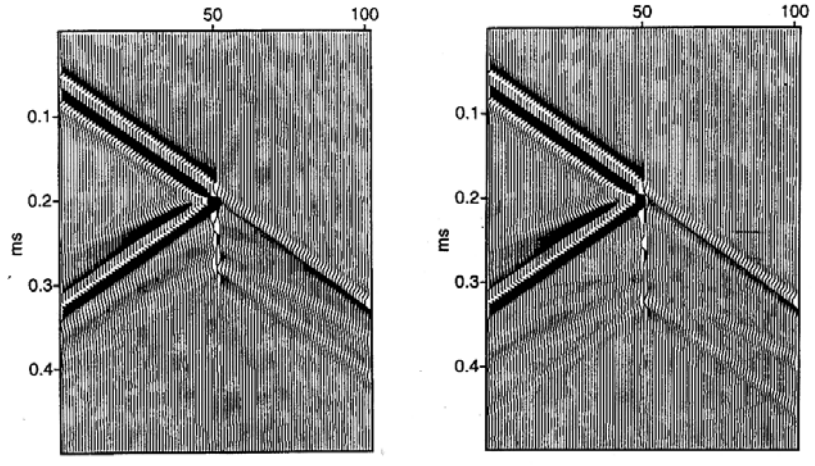

Figure 4 Same as Figure 3 with a 10-cm crack depth (left) and with a 15-cm crack depth (right)

from R-wave to body wave can be seen (Figure 3*(e)*), particularly as reflected waves (the body wave can be distinguished by its higher velocity). Note that a delayed R-wave is transmitted (Figure 3*(d)*), its time delay increasing with the crack depth (Figure 4). The time delay corresponds to the travel time of the R-wave (with a velocity of 2318 m s^{-1} calculated from *Vs* and ν) along twice the crack depth. Thus, this delayed transmitted wave is the wave which travels around the crack.

These results confirm and improve the diffraction pattern previously quoted from the ultrasonics techniques. We can identify each wave train of the model including the converted body waves. Moreover, these numerical results give information about the energy of the wave trains. Interestingly, the low energy of the delayed transmitted wave confirms that in the case of experimental signals, measuring the time delay would be difficult. Scattering from microstructures in a non-homogeneous medium produces noise which would cover this low energy wave. It appears difficult to work in the time domain to determine the crack depth.

A NDT method in the spectral domain

We propose here another way to obtain information about the crack depth. Synthetic seismograms have similar properties to the real ones as regards to their spectral content. Physically, the depth penetration of the R-wave depends on the frequency. For a surface crack, only low frequencies of the incident wave have significant energy below the crack and are therefore directly transmitted. From the spectral analysis of this directly transmitted wave and of the incident wave, a 'cut-off' frequency can be determined which is linked to the crack depth.

In the seismograms, the displacement field due to the R-waves is the most energetic. Thus, in the spectrum of a signal, the spectral features of R-waves are dominant. The reflected wave contains a lot of energy relative to the transmitted wave (Figures 3 and 4). However, the reflected wave is theoretically composed of the high frequency content of the incident wave. The presence of the reflected wave on the signal recorded before the crack would therefore amplify the high frequency band in the spectrum of the incident wave. So the 'cut-off' frequency phenomenon is not disturbed by the reflected wave. To compare the spectral features of the direct transmitted wave and the incident wave, we calculated the spectral ratio of two records selected from each side of the crack.

The results calculated from synthetic seismograms in the case of a 9-cm depth crack is presented in Figure 5. This figure shows the mean of 50 curves calculated with different couples of sensors with the same distance from one to the other. In theory, the position of the sensors relative to the crack is of no influence. The mean curve starts at a value of around 1 and drops strongly at a frequency of $\approx$ 9 kHz where it reaches a mean value of less than 0.5. For a velocity of 2318 m s^{-1}, the corresponding wavelength is about 26 cm. Because the maximum of a R-wave propagates at approximately 1/3 of the wavelength in depth, the crack depth can be evaluated at 8.6 cm (less than 5% errors compared to the actual value). Thus, this determination of a cut-off frequency gives a good evaluation of the crack depth.

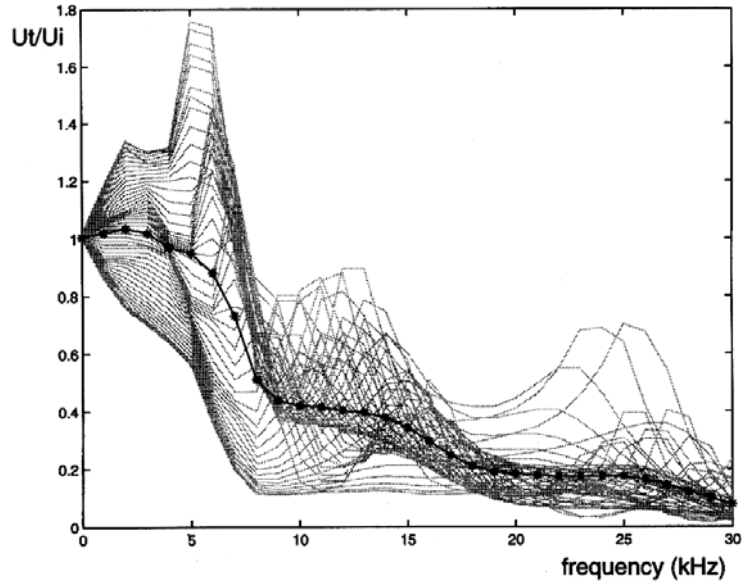

Figure 5 Mean curve of the spectral ratio of the transmitted wave on the incident wave in the case of synthetic signals

Experimental validation

Description of the experimental set-up

To validate this hypothesis, a new set of experimental tests was carried out. More sensors were used than for the previous tests and they were located at larger distances from the crack. The experimental site was a concrete slab of 6 × 4 m and a depth of 0.6 m without iron framework. On the surface of the slab, three artificial cracks were cut with a width of 5 mm and three different depth values: 4, 9 and 16 cm. Twelve sensors were placed on each side of the crack at steps of 10 cm. The source was the same as for the first tests and it was located at the boundary of the slab in order to be as far as possible from the first sensors and to avoid a first reflection on the boundary of the slab (Figure 6). We carried out the tests in two steps with five impacts on each side of the slab. Signals were stacked to improve the signal to noise ratio. They were then band filtered according to the theoretical response of the sensors and corrected for the geometrical spreading. The source location was reversed for each receiver location to get a double set of data. Figure 7 shows time domain signals and spectral amplitude of two signals after processing.

Spectral ratio evaluation process

To be able to compare the experimental and the numerical results, the spectral ratio of the transmitted wave on the incident wave must be calculated. A classical principle of calculation in geophysical signal processing was used which minimises the source effects and the influence of the different response functions of the sensors.

If A_{ij} is the amplitude in the spectral domain of a signal recorded from source i at receiver j, we can write a relation with U_{ij}, the absolute response function of the medium at location j and for a source at location i

$$A_{ij} = S_i \cdot U_{ij} \cdot R_j \tag{10}$$

where S_i is the ith source function and R_j is the response function of receiver j.

Following Equation (10), we can write (Figure 8):

$$A_{11} = S_1 \cdot U_{11} \cdot R_1 \tag{11}$$

$$A_{12} = S_1 \cdot U_{12} \cdot R_2 \tag{12}$$

$$A_{21} = S_2 \cdot U_{21} \cdot R_1 \tag{13}$$

$$A_{22} = S_2 \cdot U_{22} \cdot R_2 \tag{14}$$

We can calculates the amplitude ratio with

$$\frac{A_{12}}{A_{11}} \times \frac{A_{21}}{A_{22}} = \frac{S_1 \cdot U_{12} \cdot R_2}{S_1 \cdot U_{11} \cdot R_1} \times \frac{S_2 \cdot U_{21} \cdot R_1}{S_2 \cdot U_{22} \cdot R_2} = \frac{U_{12}}{U_{11}} \times \frac{U_{21}}{U_{22}} \tag{15}$$

identifying the common part of the path, we can write:

$$\frac{U_{12}}{U_{11}} = \frac{U_{21}}{U_{22}} \tag{16}$$

thus

$$\frac{A_{12}}{A_{11}} \times \frac{A_{21}}{A_{22}} = \left(\frac{U_{12}}{U_{11}}\right)^2 \tag{17}$$

and therefore

$$\frac{U_{12}}{U_{11}} = \sqrt{\frac{A_{12}}{A_{11}} \times \frac{A_{21}}{A_{22}}} \tag{18}$$

In this way, we have removed the source and receiver transfer functions. This process is applied to the data for each crack depth. In each case, 24 curves are calculated for different couples of sensors on each side of the crack. At the

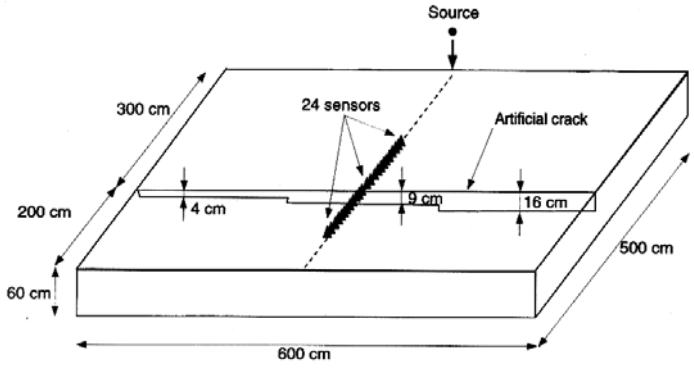

Figure 6 Schema of the experimental site with the localisation of the sensors and of the source in the case of the central crack with a depth of 9 cm

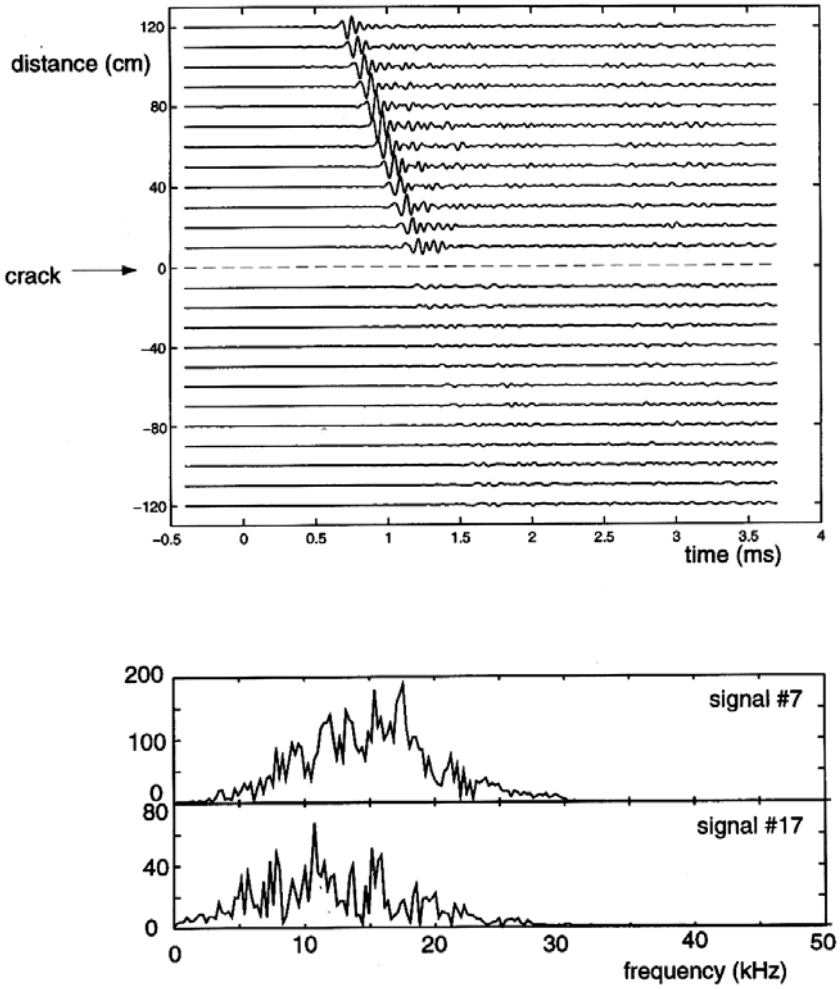

Figure 7 Experimental signals (top) obtained with the field conditions of Figure 6 and a representative example of spectra (bottom) of two signals recorded before (no. 7) and after (no. 17) the crack

end, the curves are smoothed to keep only the global aspect. The mean curves are presented in Figure 9. On the same figure, three curves calculated from our numerical model are presented.

Discussion

The first feature of this curves is the attenuation of the high frequencies. Each curve starts around 1 at 3 kHz. Below 3 kHz the experimental data cannot be taken into account: they correspond to wavelengths greater than the thickness of the slab and thus are influenced by the environmental medium. All the curves drop to values under 0.5. The decrease takes place at different frequencies depending on the crack depth. Notice that numerical and experimental curves follow the same trend, so the cut-off frequency phenomenon is verified experimentally.

A cut-off frequency can be determined as the frequency corresponding to the end of the decrease. We therefore picked three frequencies: 5.5, 9 and 17 kHz (Figure 9). These frequencies correspond to wavelengths of 42, 26 and

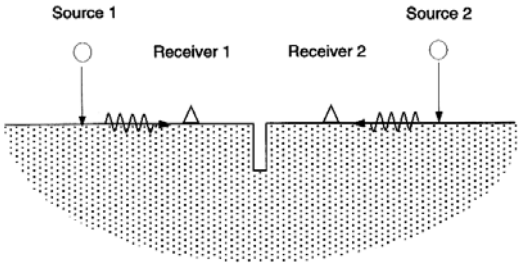

Figure 8 Schema of the reversed source location principle

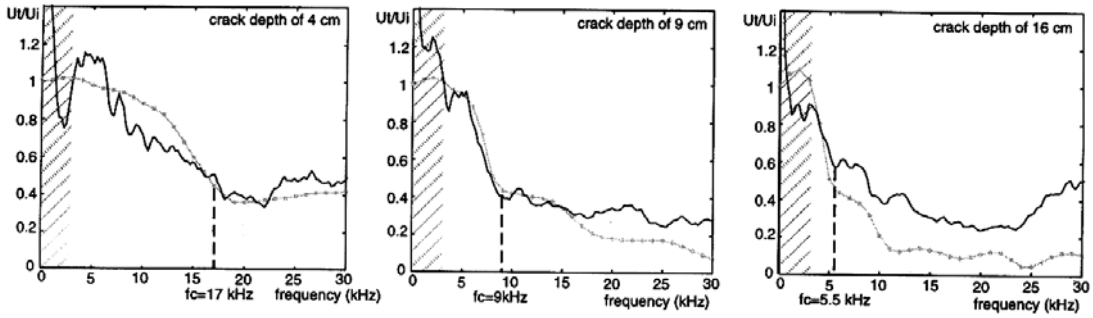

Figure 9 Spectral ratios of the transmitted on the incident waves for three different crack depths from experimental data (black curve) and numerical data (grey curves). The area of shadow on the left corresponds to wavelengths greater than the thickness of the slab

14 cm. The crack depths are therefore evaluated to be 14.0, 8.6 and 4.5 cm. The depths of the cracks found experimentally were within 15% of the actual sizes. The determination of experimental cut-off frequencies is not very accurate because the variations of the experimental curves are significant. However, the information supplied by the numerical curves makes it possible to confirm the trends of the experimental curves which helps to determine the cut-off frequencies. We are currently working to improve the accuracy of this method.

Another procedure could eventually be developed with these tools: the calculation of abacus. The numerical code makes it possible to calculate many models of a crack characterised by simple parameters such as the crack depth. Abacus could thus be established for possible crack depths and experimental curves could be adjusted to them. The evaluation of the crack depth could be greatly improved. But this hypothesis needs to be validated by more experimental work

Conclusion and perspectives

The problem of the detection and characterisation of surface cracks in structures is of paramount importance for civil engineers. Due to their great sensitivity to the propagation medium, R-waves seem to be a promising tool.

We studied a first application of this tool on an experimental site. It appears that the recorded signals were complex because of the non-homogeneity of the concrete. To improve our understanding of the behaviour of R-waves, a numerical simulation was developed. This model, adapted from an earth physic code, is based on an IBEM. It calculates the three-dimensional seismic response of two-dimensional structures. Synthetic signals were obtained for the propagation of a R-wave across various surface cracks. With these signals, a signal processing method to determine crack features, such as crack depth, is suggested. This method was verified in the field on artificial cracks in a concrete slab. Experimental and numerical results were in agreement. IBEM seems to be an efficient tool to study the diffraction of R-waves. It enabled us to design a reliable experimental procedure and can be used to improve the crack depth evaluation.

Future perspectives are to broaden the method to the case of more realistic cracks (water-filled cracks, cracks with mechanical contact between the two lips, ...). The objective is to quantify the real ability of the R-waves for the non-destructive testing of surface cracks in concrete structures.

References

1 **Sack, D. A., Olson, L. D. and Phelps, G. C.** Innovations for NDT of concrete structures: performance and prevention of deficiencies and failures. In *Mater. Eng. Congr.*, ASCE, New York, pp 519–531, 1992.

2 **Shah, S. and Landis, E.** Applications of NDT to basic and applied concrete research. In *Proceedings of International Symposium on Non-Destrutive Testing in Civil Engineering*, Vol. 1, pp. 31–38, 1995.

3 **Büyüköztürk, O.** Imaging of concrete structures. In *Proceedings of International Conference on Non-Destrutive Testing in Civil Engineering*, Vol. 1, pp. 31–52, 1997.

4 **Ditchburn, R. J., Burke, S. K. and Scala, C. M.** NDT of welds: state of the art. *NDT&E International*, 1996, **29**(2), 111–117.

5 **Aki, K. and Richards, P.G.** Quantitative seismology, W. H. Freeman, San Francisco, CA, 1980.

6 **Miller, G. F. and Pursey, H.** On the partition of energy between elastic waves in a semi-infinite solid. *Proceeding Royal Society, London, Series A*, 1955, **233**, 55–69.

7 **Parasnis, D. S.** *Principles of Applied Geophysics*, 4th ed., Sciences Paperbacks, London, p. 263, 1986.

8 **Heisey, J. S.** Stokoe II, K. H. Hudson, W. R. and Meyer A. H. Determination of in situ shear wave velocities from spectral analysis of surface waves. Research report 256-2, Center for Transportation Research, University of Texas at Austin, 1982.

9 **Nazarian, S. and Stokoe II, K. H.** In situ determination of elastic moduli of pavements systems by spectral analysis of surface waves method (practical aspect). Research report 368-1F, Center for Transportation Research, University of Texas at Austin, 1985.

10 **Jongmans, D., Campillo, M. and Demanet, D.** The use of surface wave inversion and seismic reflection methods for engineering applications, Proceedings of the sixth Congress of the International Association of Engineering Geology, pp 10, Amsterdam, 1990.

11 **Jongmans, D., Demanet, D., Horrent, C., Campillo, M. and Sànchez-Sesma, F. J.** Dynamic soil parameter determination by geophysical prospecting in Mexico City: implication for site effect modelling. *Soil Dynamics and Earthquake Engineering*, 1996, **15**, 549–559.

12 **Tittmann, B. R., Cohen-Tenoudji, F., de Billy, M., Jungman, A. and Quentin, G.** A simple approach to estimate the size of small cracks with the use of acoustic surfaces waves. *Appl. Phys. Lett.*, 1978, **33**(1), 6–8.

13 **Cooper, J. A., Crosbie, R. A., Dewhurst, R. J., McKie, A. D. W. and Palmer, S. B.** Surface acoustic wave interactions with cracks and slots: a noncontacting study using lasers. *IEEE Transactions on Ultrasonics Ferroelectrics and Frequency Control*, 1986, **UFFC-33**(5), 462–470.

14 **Burger, C. P. and Testa, A.** Rayleigh wave spectroscopy to measure the depth of surface cracks. In *Proceedings of the Thirteenth Symposium on Non Destructive Evaluation*, San Antonio, TX, 21–213 April 1981.

15 **Imram, I., Nazarian, S. and Picornell, M.** Crack detection using time domain wave propagation technique. *Jr. Geotech. Eng.*, 1995, **121**(2), 198–207.
16 **Richart, F. E., Hall, J. R. and Woods, R. D.** *Vibration of Soils and Foundations*. Prentice Hall, Englewood Cliffs, NJ, 1970.
17 **May, T. W. and Bolt, B. A.** The effectiveness of trenches in reducing seismic motion. *Earthquake Engineering and Structural Dynamics*, 1982, **10**, 195–210.
18 **Kalinski, M. E.** Measurements of intact and cracked concrete structural elements by the SASW methods. Thesis of the University of Texas at Austin, 1994.
19 **Bard, P. Y.** Diffracted waves and displacement field over two-dimensional elevated topographies. *Geophys. J.R. Astr. Soc.*, 1982, **71**, 731–760.
20 **Sànchez-Sesma, F. J.** Diffraction of elastic wave by three-dimensional surface irregularities. *Bul. Seism. Soc. Am.*, 1983, **73**, 1621–1636.
21 **Pedersen, H. A., Sanchez-Sesma, F. J. and Campillo, M.** Three-dimensional scattering by two dimensional topographies. *Bull. Seism. Soc. Am.*, 1994, **84**, 1169–1183.
22 **Sànchez-Sesma, F. J. and Campillo, M.** Topographics effects for incident P SV, and Rayleigh waves. *Tectonophysics*, 1993, **218**, 113–125.